ACS Photonics

pubs.acs.org/journal/apchd5

Article

Plasmonic Superchiral Lattice Resonances in the Mid-Infrared

Francesco Mattioli,[#] Giuseppe Mazzeo,[#] Giovanna Longhi, Sergio Abbate, Giovanni Pellegrini, Erika Mogni, Michele Celebrano, Marco Finazzi, Lamberto Duò, Chiara Giuseppina Zanchi, Matteo Tommasini, Marialilia Pea, Sara Cibella, Raffaella Polito, Filippo Sciortino, Leonetta Baldassarre, Alessandro Nucara, Michele Ortolani, and Paolo Biagioni*

Cite This: *ACS Photonics* 2020, 7, 2676–2681

Read Online

ACCESS | Metrics & More | Article Recommendations | Supporting Information

ABSTRACT: Recent efforts in the field of surface-enhanced spectroscopies have focused on the paradigm of "superchirality", entailing the engineering of the local electromagnetic fields to boost the enantiospecific interaction between light and chiral molecules. In this framework, approaches based on both metallic and dielectric nanostructures have been proposed and have also recently been extended to vibrational circular dichroism in the mid-infrared. In this work, we design, fabricate, and characterize a lattice of chiral plasmonic slits featuring enhanced chiral fields in the mid-infrared. We exploit collective lattice resonances to further enhance the local intensity and to generate sharp features in the circular dichroism spectra of the platform. Such features are ideally suited to test the superchiral coupling with the vibrational resonances of chiral molecules.

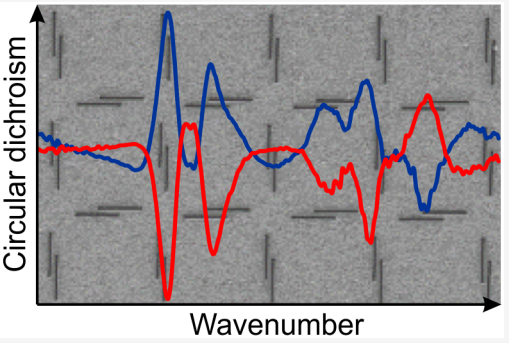

KEYWORDS: *plasmonics, mid-infrared, optical chirality, vibrational circular dichroism, lattice resonances*

Since the seminal works by Tang and Cohen,[1,2] several schemes have been developed by the nano-optics community to merge the sensitivity of surface-enhanced spectroscopies with the enantioselectivity provided by chiroptical techniques. The common goal of such "superchiral" approaches is to engineer the local electromagnetic fields by means of metallic[3−15] or dielectric[16−20] nanostructures and enhance their ability to selectively interact with chiral molecules of a specific handedness. All such attempts stem from the consideration that, in the lowest-order dipolar approximation, the dissymmetry factor for the relative absorption between left and right circularly polarized light by a molecule can be cast into the form $g = \left(\frac{G''}{\alpha''}\right)\left(\frac{2C}{\omega U_e}\right)$, where G'' and α'' are the imaginary part of the mixed and electric polarizabilities, respectively, $C = \frac{\varepsilon_0\omega}{2}(\mathbf{E}^*\cdot\mathbf{B})$ is the "optical chirality", ω is the frequency of the incident light, and U_e is the energy density associated with the electric field. While in the original proposal the term "superchiral" was specifically coined to define those field configurations that lead to a larger detected dissymmetry factor g compared to standard plane wave illumination,[1] since then it has become common practice in the literature to employ the same term to define, more generally, also all those schemes that lead to an enhanced optical chirality C.

It is fair to state that the optimal requirements for surface-enhanced chiroptical spectroscopies are not yet fully established. When plasmonic enhancement is involved in the detection scheme, two resonances naturally come into play: the localized plasmon resonance in the nanoparticles and the electronic or vibrational resonance in the chiral molecules. Most of the experimental results published so far with localized plasmons are based on chiroptical refractometric sensing in the visible spectral range, that is, on the different refractive index that characterizes nonabsorbing chiral molecules when they are illuminated off resonance by fields with opposite optical chirality. The effect of such a contrast can be observed by means of circular dichroism (CD) spectra on resonance with the localized plasmons of the system. In this approach, both chiral and nonchiral plasmonic structures have been proposed and the molecular chirality typically manifests itself via the shift and the change in the line shape induced on the plasmonic spectral features.[3,6,8,12,14] In this context, the design and simulation of coupled plasmonic-molecular chiral systems is also a very open field of research with no straightforward strategies. Recently, also racemic lattices of chiral plasmonic antennas, featuring both types of handedness in the same sample, were successfully employed.[15]

Received: February 2, 2020
Published: August 19, 2020

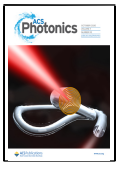

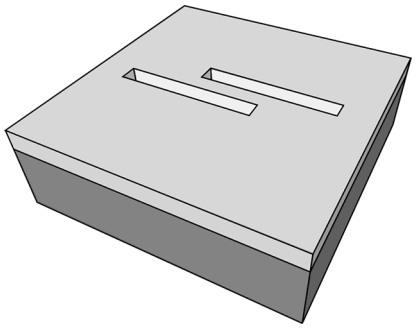

Figure 1. Sketch of the individual building block featuring two slits in a chiral configuration.

Translating plasmon-enhanced chiroptical spectroscopies to the mid-infrared region allows addressing the vibrational resonances of molecules and thus increasing the sensitivity to their conformation and configuration.[21,22] In this case, both the plasmonic platform and the molecules are illuminated on resonance, possibly giving rise to the large variety of interferential lineshapes that are generated by the two coupled oscillators and are expected to manifest themselves in the CD spectra as well.

In this work we design, fabricate, and characterize a superchiral plasmonic platform in the mid-infrared. The individual building blocks are coupled slits forming a chiral arrangement, such as those sketched in Figure 1. The two slits provide resonant enhancement of the optical chirality in the region of space right above the sample surface thanks to the favorable superposition of the respective electric and magnetic fields.[23] This system is particularly appealing for use in transmission geometry, as customary for CD experiments, since it features enhanced transmissivity in correspondence with the dipolar plasmonic resonance. However, the resonance is broad, with a quality factor of only about 5, which is typical for the dipolar resonances of linear gold antennas or slits operating in the mid-infrared. Moreover, the strong linear anisotropy of the slits gives rise to dramatic artifacts that overwhelm the genuine CD signal. In order to counterbalance these drawbacks, we design a resonant slit lattice where the superchiral response of the individual slit pairs is combined with a collective resonance giving rise to (i) enhanced superchiral near fields, (ii) narrower spectral features, and (iii) a squared arrangement that removes the linear anisotropy of the individual building blocks. In perspective, this platform is an ideal benchmark to assess the chiroptical coupling between plasmonic and molecular (vibrational) oscillators.

RESULTS AND DISCUSSION

Sample Design and Fabrication. The coupled chiral slits that represent the individual building blocks for the lattice have already been introduced in the literature previously.[23] Their specific asset is that the electric and magnetic fields associated with their fundamental electric dipole resonance superimpose in a favorable way in order to locally enhance the optical chirality. Figure 2a demonstrates the results of finite-difference time-domain (FDTD) simulations for a slit pair illuminated on resonance at 1300 cm^{-1} wavenumbers (about 7.7 μm

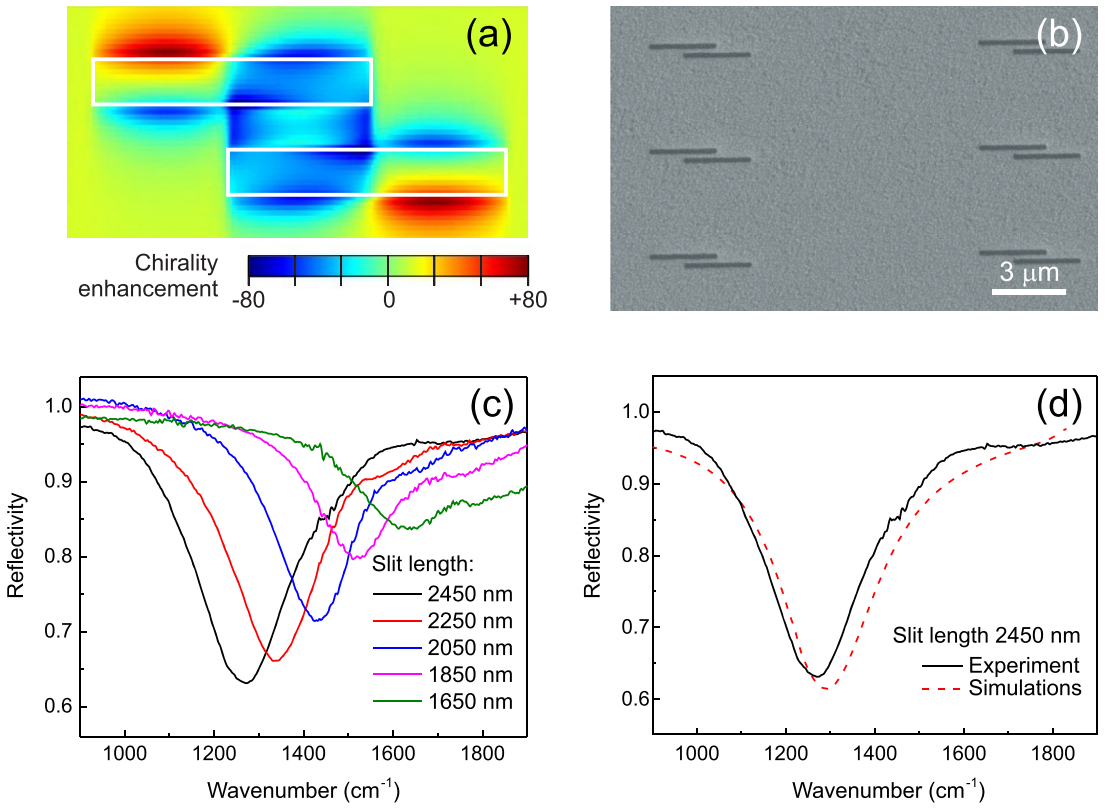

Figure 2. (a) Representative FDTD simulation of the hot spot of optical chirality created by the coupled slits; (b) representative SEM image of the fabricated slits (the widths of the slits and the gap between them are 200 and 150 nm, respectively); (c) experimental reflectivity spectra acquired from slits of different lengths (all spectra are normalized to the reflectivity of a gold mirror); (d) representative comparison between the experimental and the simulated reflectivity spectra for a length of 2450 nm of the individual slits.

https://dx.doi.org/10.1021/acsphotonics.0c00161
ACS Photonics 2020, 7, 2676−2681

wavelength). The map plots the optical chirality C defined on a plane located 10 nm above the sample surface, normalized to the optical chirality of a circularly polarized plane wave, that is, to the largest optical chirality that can be achieved by a propagating wave in the far field. A hot spot of enhanced optical chirality is indeed observed in the central part of the map.

The most investigated spectral region for VCD is roughly the 900−1800 cm^{-1} range[24] and the investigated Au slits can easily be tuned to cover the whole window by simply changing their length. We fabricate a first set of calibration samples in which the thickness of the metal film (50 nm), the width of the two slits (200 nm), and the gap between them (150 nm) are kept fixed, and only their length is varied. A representative scanning electron microscopy image of one of the samples is shown in Figure 2b. The slits are fabricated on a CaF_2 substrate using electron beam lithography (100 kV Vistec EBPG 5HR) and lift-off techniques. A negative electronic resist bilayer made of PMMA 669.06 (thickness 300 nm) and HSQ XR1541.006 (thickness 150 nm) is spun on top of the substrate and then covered with a thermally evaporated Al layer (thickness 5 nm) to prevent charging effects during exposure. After exposure and development, the slit geometry is defined on the HSQ layer and an oxygen-based reactive ion etching is used to remove the PMMA underneath and obtain the correct bilayer profile needed to perform a nanometric lift-off process. Finally, a 10 nm/40 nm Ti/Au layer is grown by electron-gun evaporation and then lifted off. The samples extend over areas of about 300 × 300 μm^2 and are characterized by means of Fourier-transform IR (FTIR) microscopy, employing an IR microscope based on a cassegrain objective in reflection geometry, with linear electric field polarization perpendicular to the long axis of the slit. The experimental results in Figure 2c confirm the wide tunability of the fundamental localized plasmon resonance (observed as a dip in the reflected signal) and are reproduced with excellent agreement by simulations with the FDTD method,[25] as demonstrated in Figure 2d, which are performed under plane-wave illumination with n = 1.35 refractive index for the CaF_2 substrate and the Au dielectric constant taken from the literature.[26]

However, when it comes to CD measurements, this design has the disadvantage of strong linear optical anisotropy, which introduces dramatic well-known artifacts in the measurement of a CD spectrum. In particular, any slight misalignment of the optical path (typically, a slightly off-normal incidence) combined with the presence of a uniaxial anisotropy in the plane of the sample surface creates the conditions for what has also been referred to as "extrinsic chirality" in the literature, an effect that can easily overwhelm any genuine CD signal.[27−29]

For this reason, we design a modified sample geometry in which the chiral slit pairs are arranged in a square lattice, as shown in Figure 3a. By doing this, we also take advantage of the closely packed arrangement to tune the lattice resonances in the system so they coherently excite the localized resonances of the nanostructures in the lattice. This spectral overlap is accompanied by strong local near fields, which have already been exploited in the literature, for example, for sensing or emission enhancement,[30,31] and by discontinuities in the reflection/transmission spectra (associated with the so-called Wood-Rayleigh anomalies) that create sharp spectral features. We fabricated a large-area sample of 5 × 5 mm^2 with a square lattice having 6 μm pitch and 2.5 μm slit length and we

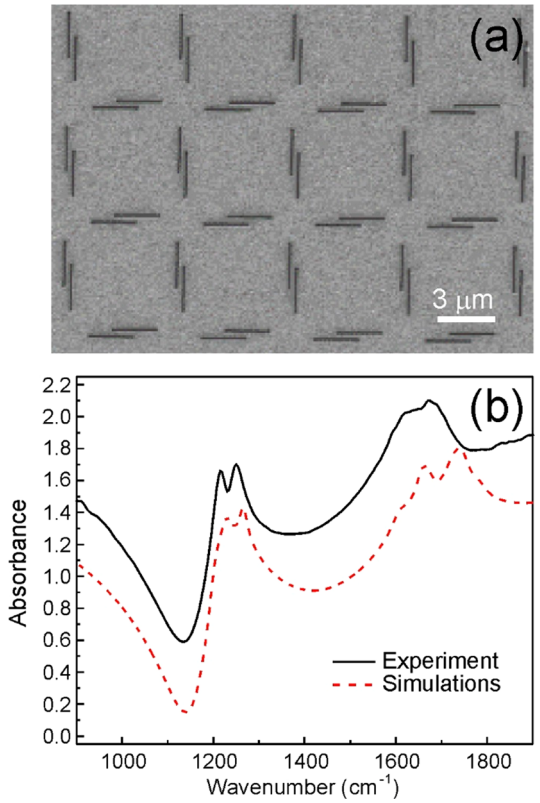

Figure 3. (a) Representative SEM image of the square slit array with a 6 μm pitch (the widths of the slits and the gap between them are 200 and 150 nm, respectively, as in the previous case); (b) Absorbance FTIR spectrum acquired with a quasi-collimated source and the associated RCWA simulations obtained by averaging over an angular range of ±2°.

characterized it by FTIR spectroscopy. The lattice pitch was chosen in order to match the localized slit resonance with one of the expected lattice resonances (specifically, with the one associated with interslit coupling via diffracted waves traveling parallel to the side of the square cell inside the substrate, as discussed below) and to locate the other main lattice resonances within the spectral range of interest for VCD. In order to experimentally achieve quasi-plane wave illumination by still using the noncollimated broadband blackbody source of the FTIR spectrometer, we have introduced an iris aperture in the FTIR setup at a distance of L = 120 mm before the focal sample position. By closing this iris from the original beam diameter of about 30 mm down to a diameter of about 4 mm, that is, smaller than the sample size, we could probe the sample with a quasi-collimated beam with residual cone angle distribution of about ±1° (whereas ±7° is typical for standard FTIR spectrometers). With our collection geometry in the forward direction we probe the zeroth diffraction order, while the periodicity of the square lattice sets the appearance of the first order in air around 1666 cm^{-1} and of the first order in the CaF_2 substrate around 1235 cm^{-1}. Moreover, the diagonal of the square unit cell, which is about 8.5 μm, further contributes to the overall response by opening the possibility for a diffraction order in air around 1160 cm^{-1}. As is typical for lattice resonances, the appearance of such diffraction orders strongly affects the coupling between the slits in the lattice and determines sharp features/discontinuities in transmission and reflection spectra. Indeed, the transmission spectrum (Figure

https://dx.doi.org/10.1021/acsphotonics.0c00161
ACS Photonics 2020, 7, 2676−2681

3b), clearly reveals a more complex response than the one displayed by the uniaxial array, with narrower lineshapes and sharp features marking the discontinuities introduced by the diffraction orders. Noticeably, the experimental line widths are limited by the residual cone angle distribution, which, as expected, broadens any feature associated with grating effects.[32] For sake of clarity, it should be noted that such transmission spectra are here expressed and labeled as "absorbance", as customary for CD measurements, although no significant absorption is present for gold plasmonic nanostructures in the mid-infrared and light is mainly either reflected or transmitted by the system. To avoid convergence problems that typically affect time-domain methods applied to structures endowed with sharp resonances, this sample is modeled by employing the rigorous coupled-wave analysis (RCWA), a frequency-domain method that is particularly suited for periodic systems.[33] In order to mimic the residual cone angle distribution of the FTIR experiment with quasi-collimated beams, we run separate plane-wave simulations for different angles of incidence and we then sum them to construct the final transmission spectrum: we have found that a theoretical residual cone angle distribution of ±2° fairly reproduces the experimental results, a slight deviation from the ±1° expected from purely geometrical considerations. The simulated and measured spectra in Figure 3b display a fair agreement in the entire molecular fingerprint range 900−1900 cm^{-1}. Details of these calculations, together with simulated intensity and optical chirality maps, are reported in the Supporting Information.

Chiroptical Characterization. The CD spectrum of the plasmonic lattice is investigated with a JASCO FVS6000 apparatus, which is equipped with a high intensity ceramic source, a MCT-V (HgCdTe) diode detector, and a ZnSe photoelastic modulator for the lock-in acquisition of CD spectra. We study two samples characterized by opposite handedness of the individual slit pairs. To confirm that the measurements are reasonably free from artifacts, possibly induced by the planar two-dimensional geometry of the sample, as discussed above, we acquire the VCD spectra as a function of the azimuthal angle. Figure 4a displays a set of measurements acquired for the two plasmonic enantiomers (black and red curves, respectively). The results confirm that (i) the sharp spectral features of the sample transmissivity translate into sharp CD lineshapes; (ii) the CD spectra from the two enantiomers are the mirror image of each other, as expected; and (iii) the measurements are reasonably free from artifacts, as demonstrated by the fair reproducibility of the spectra collected at different azimuthal angles. The presence of the sharp features in the CD spectrum, in particular, is appealing in view of sensing schemes in which the coupling between the plasmonic and the molecular vibrational oscillators is exploited and analyzed. It should be stressed that, for such two-dimensional chiral systems, it is expected that the CD spectrum is also reversed upon flipping the sample with respect to the direction of light propagation.[34] This is confirmed by the measurements in Figure 4b, in which the black spectra are the same as those in Figure 4a, while the red spectra are acquired from the same flipped plasmonic enantiomer.

It should be noted here that, with the available computational resources and because of the already mentioned high quality factors of the lattice resonances under investigation, we have not been able to reach the convergence accuracy required

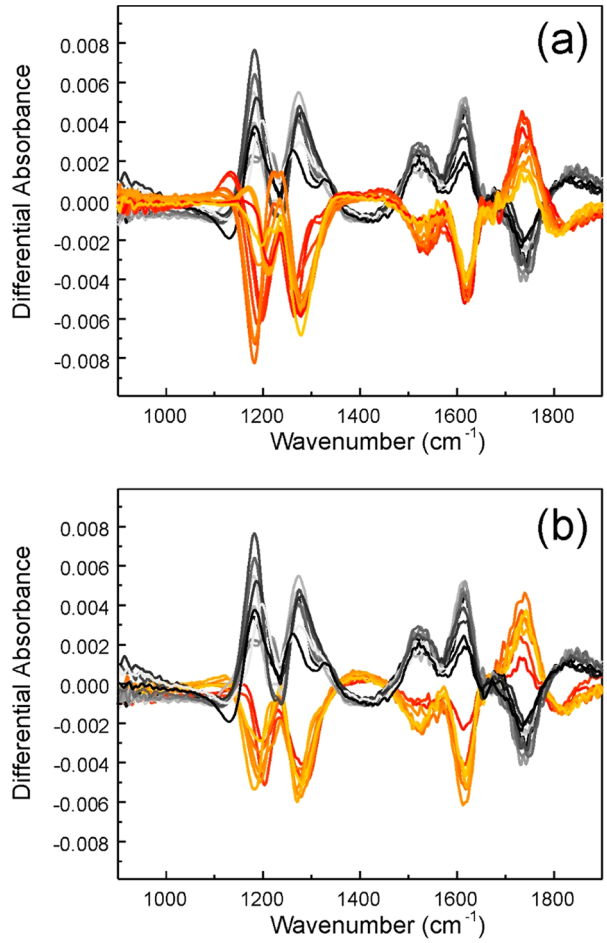

Figure 4. (a) CD spectra acquired for two opposite plasmonic enantiomers (black and red lines, respectively) for different azimuthal angles in steps of 20°; (b) CD spectra acquired for the same plasmonic enantiomer after flipping the sample with respect to the propagation direction of the excitation beam (black and red lines, respectively, the black lines represent the same data as those in panel (a) for different azimuthal angles in steps of 20°). Line colors from lighter to darker correspond to azimuthal angles from 0° to 180°.

to successfully reproduce the experimental VCD spectra. Nevertheless, we provide in Figure 5 a representative map for

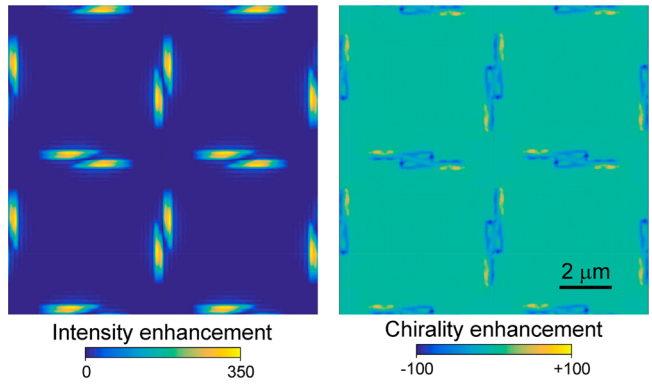

Figure 5. Intensity and optical chirality enhancement maps calculated for the plasmonic lattice on a plane located 10 nm above the sample surface, under circularly polarized illumination, at correspondence with the main simulated transmission resonance, around 1130 cm^{-1}. Normal incidence is considered here.

https://dx.doi.org/10.1021/acsphotonics.0c00161
ACS Photonics 2020, 7, 2676−2681

the local optical chirality enhancement computed from the simulations already discussed in Figure 3b. We focus here our attention on the strongest transmission resonance around 1130 cm^{-1}, which is the one providing the largest enhancement within the investigated spectral range. A more comprehensive collection of local maps computed for several frequencies is provided in the Supporting Information.

CONCLUSIONS

In conclusion, we have designed, fabricated, and characterized a lattice of chiral slit pairs, featuring superchiral near fields whose intensity and spectral response is enriched by the presence of lattice resonances in the system, resulting in narrow plasmonic CD lineshapes. The plasmonic lattice represents an ideal system for surface-enhanced vibrational CD in transmission geometry, thanks to the resonantly enhanced transmissivity through the slits. Along this line, the system represents an ideal benchmark to test the chiroptical coupling between localized plasmon resonances, lattice resonances, and molecular vibrational resonances of chiral molecules. Moreover, the design is viable to be modified in order to achieve an overall achiral plasmonic response by suitably alternating left and right slit pairs, thus, increasing the sensitivity to the molecular response without an overwhelming plasmonic response, as recently proposed in ref 15.

ASSOCIATED CONTENT

Supporting Information

The Supporting Information is available free of charge at https://pubs.acs.org/doi/10.1021/acsphotonics.0c00161.

Results of RCWA simulations encompassing extinction spectra, intensity enhancement maps, and chirality enhancement maps (PDF)

AUTHOR INFORMATION

Corresponding Author

Paolo Biagioni − *Dipartimento di Fisica, Politecnico di Milano, 20133 Milano, Italy;* orcid.org/0000-0003-4272-7040; Email: paolo.biagioni@polimi.it

Authors

Francesco Mattioli − *Istituto di Fotonica e Nanotecnologie - CNR, 00156 Roma, Italy*

Giuseppe Mazzeo − *Dipartimento di Medicina Molecolare e Traslazionale, Università degli Studi di Brescia, 25123 Brescia, Italy;* orcid.org/0000-0002-3819-6438

Giovanna Longhi − *Dipartimento di Medicina Molecolare e Traslazionale, Università degli Studi di Brescia, 25123 Brescia, Italy; Istituto Nazionale di Ottica − CNR, Brescia Research Unit, c/o CSMT, 25123 Brescia, Italy;* orcid.org/0000-0002-0011-5946

Sergio Abbate − *Dipartimento di Medicina Molecolare e Traslazionale, Università degli Studi di Brescia, 25123 Brescia, Italy; Istituto Nazionale di Ottica − CNR, Brescia Research Unit, c/o CSMT, 25123 Brescia, Italy;* orcid.org/0000-0001-9359-1214

Giovanni Pellegrini − *Dipartimento di Fisica, Politecnico di Milano, 20133 Milano, Italy;* orcid.org/0000-0003-0105-3449

Erika Mogni − *Dipartimento di Fisica, Politecnico di Milano, 20133 Milano, Italy*

Michele Celebrano − *Dipartimento di Fisica, Politecnico di Milano, 20133 Milano, Italy;* orcid.org/0000-0003-3336-3580

Marco Finazzi − *Dipartimento di Fisica, Politecnico di Milano, 20133 Milano, Italy;* orcid.org/0000-0002-9197-3654

Lamberto Duò − *Dipartimento di Fisica, Politecnico di Milano, 20133 Milano, Italy*

Chiara Giuseppina Zanchi − *Dipartimento di Chimica, Materiali e Ingegneria Chimica, Politecnico di Milano, 20133 Milano, Italy*

Matteo Tommasini − *Dipartimento di Chimica, Materiali e Ingegneria Chimica, Politecnico di Milano, 20133 Milano, Italy;* orcid.org/0000-0002-7917-426X

Marialilia Pea − *Istituto di Fotonica e Nanotecnologie - CNR, 00156 Roma, Italy*

Sara Cibella − *Istituto di Fotonica e Nanotecnologie - CNR, 00156 Roma, Italy*

Raffaella Polito − *Dipartimento di Fisica, Sapienza Università di Roma, 000185 Roma, Italy*

Filippo Sciortino − *Dipartimento di Fisica, Sapienza Università di Roma, 000185 Roma, Italy*

Leonetta Baldassarre − *Dipartimento di Fisica, Sapienza Università di Roma, 000185 Roma, Italy;* orcid.org/0000-0003-2217-0564

Alessandro Nucara − *Dipartimento di Fisica, Sapienza Università di Roma, 000185 Roma, Italy*

Michele Ortolani − *Dipartimento di Fisica, Sapienza Università di Roma, 000185 Roma, Italy;* orcid.org/0000-0002-7203-5355

Complete contact information is available at: https://pubs.acs.org/10.1021/acsphotonics.0c00161

Author Contributions

#F.M. and G.M. contributed equally to this work.

Notes

The authors declare no competing financial interest.

ACKNOWLEDGMENTS

We acknowledge the kind support of Philippe Lalanne in the use of the RETICOLO software and the contribution of Francesco Rusconi to the discussion of the experimental results. The research leading to these results has received funding from the Italian Ministry of Education, University, and Research (MIUR), PRIN Project "Plasmon-enhanced vibrational circular dichroism", ID 2015FSHNCB.

REFERENCES

(1) Tang, Y.; Cohen, A. E. Optical Chirality and Its Interaction with Matter. *Phys. Rev. Lett.* **2010**, *104*, 163901.

(2) Tang, Y.; Cohen, A. E. Enhanced Enantioselectivity in Excitation of Chiral Molecules by Superchiral Light. *Science* **2011**, *332*, 333−336.

(3) Hendry, E.; Carpy, T.; Johnston, J.; Popland, M.; Mikhaylovskiy, R. V.; Lapthorn, A. J.; Kelly, S. M.; Barron, L. D.; Gadegaard, N.; Kadodwala, M. Ultrasensitive detection and characterization of biomolecules using superchiral fields. *Nat. Nanotechnol.* **2010**, *5*, 783−787.

(4) Govorov, A. O.; Fan, Z.; Hernandez, P.; Slocik, J. M.; Naik, R. R. Theory of Circular Dichroism of Nanomaterials Comprising Chiral Molecules and Nanocrystals: Plasmon Enhancement, Dipole Interactions, and Dielectric effects. *Nano Lett.* **2010**, *10*, 1374−1382.

(5) Govorov, A. O.; Fan, Z. Theory of Chiral Plasmonic Nanostructures Comprising Metal Nanocrystals and Chiral Molecular Media. *ChemPhysChem* **2012**, *13*, 2551−2560.

(6) Abdulrahman, N. A.; Fan, Z.; Tonooka, T.; Kelly, S. M.; Gadegaard, N.; Hendry, E.; Govorov, A. O.; Kadodwala, M. Induced Chirality through Electromagnetic Coupling between Chiral Molecular Layers and Plasmonic Nanostructures. *Nano Lett.* **2012**, *12*, 977−983.
(7) Frank, B.; Yin, X.; Schäferling, M.; Zhao, J.; Hein, S. M.; Braun, P. V.; Giessen, H. Large-Area 3D Chiral Plasmonic Structures. *ACS Nano* **2013**, *7*, 6321−6329.
(8) Lu, F.; Tian, Y.; Liu, M.; Su, D.; Zhang, H.; Govorov, A. O.; Gang, O. Discrete Nanocubes as Plasmonic Reporters of Molecular Chirality. *Nano Lett.* **2013**, *13*, 3145−3151.
(9) Valev, V. K.; Baumberg, J. J.; Sibilia, C.; Verbiest, T. Plasmonic Nanostructures: Chirality and Chiroptical Effects in Plasmonic Nanostructures: Fundamentals, Recent Progress, and Outlook. *Adv. Mater.* **2013**, *25*, 2509.
(10) Valev, V. K.; Baumberg, J. J.; De Clercq, B.; Braz, N.; Zheng, X.; Osley, E. J.; Vandendriessche, S.; Hojeij, M.; Blejean, C.; Mertens, J.; et al. Nonlinear Superchiral Meta- Surfaces: Tuning Chirality and Disentangling Non-Reciprocity at the Nanoscale. *Adv. Mater.* **2014**, *26*, 4074−4081.
(11) Schäferling, M.; Yin, X.; Engheta, N.; Giessen, H. Helical Plasmonic Nanostructures as Prototypical Chiral Near-Field Sources. *ACS Photonics* **2014**, *1*, 530−537.
(12) Tullius, R.; Karimullah, A. S.; Rodier, M.; Fitzpatrick, B.; Gadegaard, N.; Barron, L. D.; Rotello, V. M.; Cooke, G.; Lapthorn, A.; Kadodwala, M. Superchiral" Spectroscopy: Detection of Protein Higher Order Hierarchical Structure with Chiral Plasmonic Nanostructures. *J. Am. Chem. Soc.* **2015**, *137*, 8380−8383.
(13) Nesterov, M. L.; Yin, X.; Schäferling, M.; Giessen, H.; Weiss, T. The Role of Plasmon-Generated Near Fields for Enhanced Circular Dichroism Spectroscopy. *ACS Photonics* **2016**, *3*, 578−583.
(14) Zhao, Y.; Askarpour, A. N.; Sun, L.; Shi, J.; Li, X.; Alù, A. Chirality detection of enantiomers using twisted optical metamaterials. *Nat. Commun.* **2017**, *8*, 14180.
(15) García-Guirado, J.; Svedendahl, M.; Puigdollers, J.; Quidant, R. Enantiomer-selective molecular sensing using racemic nanoplasmonic arrays. *Nano Lett.* **2018**, *18*, 6279−6285.
(16) García-Guirado, J.; Svedendahl, M.; Puigdollers, J.; Quidant, R. Enhanced chiral sensing with dielectric nanoresonators. *Nano Lett.* **2020**, *20*, 585−591.
(17) Pellegrini, G.; Finazzi, M.; Celebrano, M.; Duò, L.; Biagioni, P. Chiral surface waves for enhanced circular dichroism. *Phys. Rev. B: Condens. Matter Mater. Phys.* **2017**, *95*, 241402.
(18) Pellegrini, G.; Finazzi, M.; Celebrano, M.; Duò, L.; Biagioni, P. Surface-enhanced chiroptical spectroscopy with superchiral surface waves. *Chirality* **2018**, *30*, 883−889.
(19) Mohammadi, E.; Tsakmakidis, K. L.; Askarpour, A. N.; Dehkhoda, P.; Tavakoli, A.; Altug, H. Nanophotonic platforms for enhanced chiral sensing. *ACS Photonics* **2018**, *5*, 2669−2675.
(20) García-Etxarri, A.; Dionne, J. A. Surface-enhanced circular dichroism spectroscopy mediated by nonchiral nanoantennas. *Phys. Rev. B: Condens. Matter Mater. Phys.* **2013**, *87*, 235409.
(21) Knipper, R.; Mayerhöfer, T. G.; Kopecký, V.; Huebner, U.; Popp, J. Observation of giant infrared circular dichroism in plasmonic 2D-metamaterial arrays. *ACS Photonics* **2018**, *5*, 1176−1180.
(22) Knipper, R.; Kopecký, V.; Huebner, U.; Popp, J.; Mayerhöfer, T. G. Slit-enhanced chiral- and broadband infrared ultra-sensing. *ACS Photonics* **2018**, *5*, 3238−3245.
(23) Hendry, E.; Mikhaylovskiy, R. V.; Barron, L. D.; Kadodwala, M.; Davis, T. J. Chiral Electromagnetic Fields Generated by Arrays of Nanoslits. *Nano Lett.* **2012**, *12*, 3640−3644.
(24) Nafie, L. A. *Vibrational Optical Activity - Principles and Applications*; Wiley: NY, 2011.
(25) *FDTD Solutions*; Lumerical Inc., Canada.
(26) Olmon, R. L.; Slovick, B.; Johnson, T. W.; Shelton, D.; Oh, S.-H.; Boreman, G. D.; Raschke, M. B. Optical Dielectric Function of Gold. *Phys. Rev. B: Condens. Matter Mater. Phys.* **2012**, *86*, 235147.
(27) Drezet, A.; Genet, C.; Laluet, J.-Y.; Ebbesen, Th. W. Optical chirality without optical activity: how surface plasmons give a twist to light. *Opt. Express* **2008**, *16*, 12559−12570.
(28) Plum, E.; Liu, X.-X.; Fedotov, V. A.; Chen, Y.; Tsai, D. P.; Zheludev, N. I. Metamaterials: optical activity without chirality. *Phys. Rev. Lett.* **2009**, *102*, 113902.
(29) Sersic, I.; van de Haar, M. A.; Arango, F. B.; Koenderink, A. F. Ubiquity of optical activity in planar metamaterial scatterers. *Phys. Rev. Lett.* **2012**, *108*, 223903.
(30) Adato, R.; Yanik, A. A.; Amsden, J. J.; Kaplan, D. L.; Omenetto, F. G.; Hong, M. K.; Erramilli, S.; Altug, H. Ultra-sensitive vibrational spectroscopy of protein monolayers with plasmonic nanoantenna arrays. *Proc. Natl. Acad. Sci. U. S. A.* **2009**, *106*, 19227−19232.
(31) Giannini, V.; Vecchi, G.; Gómez Rivas, J. Lighting up multipolar surface plasmon polaritons by collective resonances in arrays of nanoantennas. *Phys. Rev. Lett.* **2010**, *105*, 266801.
(32) Baldassarre, L.; Ortolani, M.; Nucara, A.; Maselli, P.; Di Gaspare, A.; Giliberti, V.; Calvani, P. Intrinsic linewidth of the plasmonic resonance in a micrometric metal mesh. *Opt. Express* **2013**, *21*, 15401−15408.
(33) Hugonin, J. P.; Lalanne, P. *Reticolo Software for Grating Analysis*; Institut d'Optique, Orsay, France, 2005.
(34) Fedotov, V. A.; Schwanecke, A. S.; Zheludev, N. I.; Khardikov, V. V.; Prosvirnin, S. L. Asymmetric transmission of light and enantiomerically sensitive plasmon resonance in planar chiral nanostructures. *Nano Lett.* **2007**, *7*, 1996−1999.

https://dx.doi.org/10.1021/acsphotonics.0c00161
ACS Photonics 2020, 7, 2676−2681